

RESEARCH

Open Access



The effect of slope height and angle on the safety factor and modes of failure of 3D slopes analysis using limit equilibrium method

Sumit Kumar^{1*} , Shiva Shankar Choudhary¹ and Avijit Burman¹

Abstract

Background It is a well-known fact that the safety of slopes majorly depends on several factors such as geometry, soil properties. The safety factor might change significantly depending on the soil type and the slope's shape. The knowledge of the nature of the change in the safety factor due to the change in the slope's height and angle is essential for implementing an effective strategy of increasing the safety factor for any slope stability problem. The influence of geometric shapes on the stability of the slope needs to be properly investigated through three-dimensional slope stability analysis, as the three-dimensional analysis is suitable for all slopes, even those which invalidate the plane-strain conditions.

Results To calculate the three-dimensional safety factor, multiple analyses of three homogenous soil slopes with different soil properties were conducted by varying slope height, angle, and combinations. Each slope's height and angle were recorded to identify the types of slope failure. The analysis's findings showed that while a decrease in height raises the safety factor nonlinearly, a decrease in slope angle increases the safety factor almost linearly. Base failure is the most likely failure for slopes with a height less than 4.0 m and an angle of inclination less than 18°. On clay and sandy clay soils, toe slide is the most common type of slope failure. The expected failure type will be either toe or face failure when the slope's height and base angle exceeds 5.0 m and 22°, respectively. This study also found that the three-dimensional safety factor for soil slope is generally 10–20% higher than the two-dimensional factor of slope safety.

Conclusions The slope's nature depended on the soil type and slope form, but the safety factor increased as the slope angle and height decreased. To determine the most efficient method for slope stabilization, it is necessary to do an extensive study on slope height and angle reduction techniques. It should be ensured that the sliding mass of soil does not rise, resulting in a potential slope failure. The present study will help identify the correlation between the height and base inclination of the slope with the expected nature of slope failure. The present study helps to investigate the variation of the safety factor of a three-dimensional homogenous soil slope subjected to self-weight only. The study can be further extended to observe the variation of the factor of safety for a 3D slope subjected to pore water pressure and seismic loading also.

Keywords Safety factor, Bishop simplified method, Digital elevation model, Slope height, Slope angle

*Correspondence:

Sumit Kumar
sumitk.phd19.ce@nitp.ac.in

¹ Department of Civil Engineering, National Institute of Technology Patna, Patna, Bihar 800005, India

1 Background

In numerous civil engineering projects, slope stability issues are ubiquitous and pervasive. Large and significant constructions like tunnels, dams, and highways are especially susceptible to slope stability problems [1]. The instability of a slope can result in enormous social and

financial losses. Roads, embankment cuts, fills, and dams must be investigated with due care to ensure the project's safety. Slopes should be adequately inspected and fixed so that they do not fall apart in a way that causes a disaster. Failures of slopes rely on soil type, geometry, soil stratification, groundwater, and infiltration [2, 3]. Failure of a slope can be caused by translational slide, rotational slide, or flow [4, 5]. Fine-grained and homogenous soils are prone to rotational slides, as shown in Fig. 1. In the analysis of soil slopes, the limit equilibrium method (LEM), limit analyses (LA), and finite element method (FEM) are the most often used methods [6]. In slope analysis, limit equilibrium approaches are widely used to establish the slope factor of safety (FS) against failure [7–12]. Initially, the stability checks of a slope were formulated in two dimensions (2D) under the assumption that plane-strain conditions prevailed. But the plane-strain assumption is often wrong when the section changes along the slope's longitudinal direction. Singh et al. [13] conducted a comprehensive analysis of conventional and soft computing techniques for slope stability analysis. In these cases, a three-dimensional (3D) slope stability study is needed to determine how the slope will fail [14]. A few scholars have developed a limit equilibrium theory-based 3D slope stability study [15–19]. The collapsing mass is symmetrical and divided into vertical columns. Researchers reported 3D method-of-columns techniques based on a symmetrical plane for failure mass [16, 20–25]. Recently Rao et al. [18] studied the Box Search technique for 3D Slope Stability Analysis Using the LEM based on the symmetric plane. Some formulations based on limit equilibrium techniques did not use a symmetrical plane [26–28]. Since [29], other scholars [30–32] have used LEM to solve the FS of asymmetrical slopes [33, 34]. presented a comprehensive literature study involving slope stability analysis.

With limit analysis, slope analysis is looked at regarding energy balance, and the results are accurate. The upper bound LA looks for the slope failure mechanism by making an acceptable velocity field from a kinetic point of view [35]. The upper bound theorem of LA is used to evaluate slope stability because no assumptions regarding interaction forces and specified failure surfaces are necessary [36–39]. Limit finite element analysis (LFEA)

was also utilized to investigate the topic of slope stability. Numerous studies have accounted for slopes' complex geometry and constitutive links [40, 41]. The lower bound theorem is attractive because it provides a reliable estimate of the load capacity of a structure by assuming a stiff plastic material model with an associated flow rule. Most numerical implementations of the lower bound theorem are based on discretizing the continuum using finite elements. Using the LA method's upper bound, many researchers have done 3D slope stability analyses [42, 43]. The displacement finite element method (FEM) and finite difference analysis (FDA), which are preferable for deformation investigations, have also been applied to slope stability evaluation based on the strength reduction method [44, 45].

The search procedure given by [29] for locating the critical failure surface (CFS) and corresponding minimum FS is compatible with other well-known column techniques, as demonstrated by [22]. Previously, the 3D simplified Janbu approach [46] was utilized to develop an efficient search strategy for locating important slip surfaces. Horizontal and vertical force equilibrium conditions were satisfied by Ugai's 3D Janbu method. Consequently, it was discovered that critical slip surfaces reported using the 3D Janbu method were significantly deeper than those found using variational formulations [47] in a number of situations, particularly for slopes in cohesive soil with low friction. In addition, the 3D simplified Janbu technique produced minimum safety factor values that were more conservative than variational solutions.

Sustainability concepts are in Policy 418 of the American Society of Civil Engineers. "Do the Right Project; Do the Project Right; Perform Life Cycle Assessment from Planning to Reuse; Use Resources Wisely; Plan for Resiliency and Validate Application of Principles" are the policies for civil engineers [48]. This motto highlights the need for project safety analysis. Adding support structures and modifying slope geometry can increase slope stability. This research aims to study the height, angle parameters and mode of failure surface for a 3D slope using LEM. Slope safety can be increased by decreasing slope height/angle; however, the safety depends on the soil type. The strategy of reducing the slope angle is more efficient for some soils than decreasing slope height,

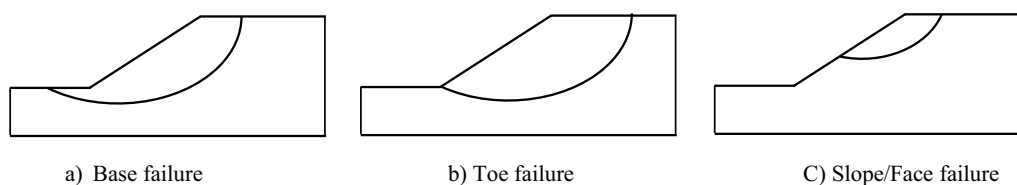


Fig. 1 Different forms of rotating slope failure

whereas the opposite is true for others. The failure mass may change if the safety factor is raised by lowering the slope height or angle. Slope height and angle's effects on the 3D FS and a 3D soil slope failure are highlighted in this study using LEM.

2 Methodology

2.1 Aim, design, and setting of the study

2.1.1 Aim

This research aims to study the height, angle parameters, and mode of failure surface for a 3D slope using LEM. The safety factor might change significantly depending on the soil type and the slope's shape. The knowledge of the nature of the change in the safety factor due to the change in the slope's height and angle is essential for implementing an effective strategy of increasing the safety factor for any slope stability problem.

2.1.2 Design

This study uses 3D slope stability analyses using the limit equilibrium method. For 3D slope stability, investigations were carried out using the Scoops3D source program. Scoops3D allows Ordinary and Bishop simplified methods to compute the FS, but in this research work, Bishop's simplified method is used for chosen problem.

2.1.3 Setting of the study

This study investigates the critical failure surface and safety factor for different heights and base inclination angle combinations for three types of soils: clayey, sandy clay, and sandy soil. To produce the 3D geometric profile of the slope, a digital elevation model (DEM) input file is prepared. The horizontal resolution of the DEM grid (m) is taken at 0.50 m intervals. An initial height variation is performed in this study to determine the mode of failure surface and safety factor. The second analytical approach involves gradually changing the slope angle while maintaining the slope height and soil characteristics constant. In a third analysis, the author investigated different slope height and angle combinations while keeping the soil parameters the same.

2.2 Geometric design of 3D soil slope

Scoops3D is a software from USGS (United States Geological Society) that can perform three-dimensional slope stability analysis. Scoops3D analyses slope stability by extending the traditional 2D limit equilibrium formulation to three dimensions. It computes the stability of a stiff soil mass covered by the spherical trial surfaces (potential sliding surfaces). For three-dimensional analysis, the entire slope domain is divided into several columns, as shown in Fig. 2. The partial columns for which at least two sides fall inside the failure surface

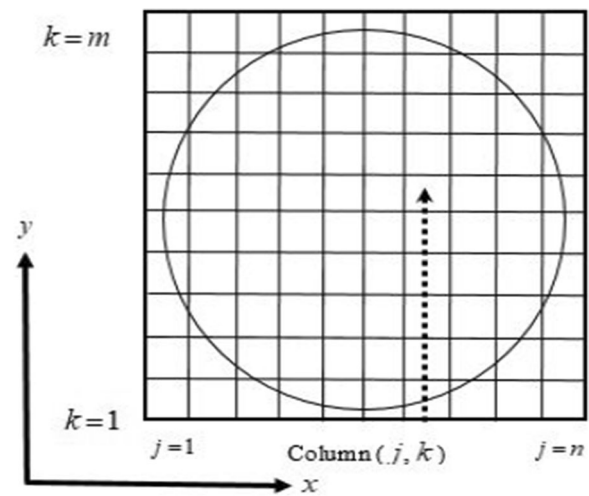


Fig. 2 Planar view of the potential sliding mass of divided columns for a 3D slope

are considered while estimating the failure mass. If partial columns are considered while calculating the failure mass, the final output results' accuracy is better [49]. The column width, also known as DEM cell size, is given as input by the user. The DEM data includes the slope surface's top elevation (i.e., z coordinate). The geometry data of any intermediate layer inside the slope are also specified in the DEM file. The average of the four surrounding DEM cell heights is used to calculate column corner elevations. The piezometric surface profile, if any, also needs to be defined using a DEM input file.

2.3 3D formulation of bishop simplified analysis

In this research, the FS of a 3D slope is determined using a Scoops3D-based computer program. Scoops3D utilizes Ordinary and Bishop simplified methods (BSM) to compute FS, but in this research work, Bishop's simplified method is used for the chosen problem. Figure 3 represents the free body diagram of the j,k column as no external force was acting on the column subjected to all possible combinations of forces.

Where W is the weight of the column; $E_{x,j,k}$, $E_{y,j,k}$ = x and y directions inter-column normal force; $H_{x,j,k}$, $H_{y,j,k}$ = Horizontal shear force in $y-z$ plane; $X_{x,j,k}$, $X_{y,j,k}$ = Inter-column shear force in $x-z$ plane; $N_{j,k}$, $U_{j,k}$ = effective normal force and base pore water force; $S_{j,k}$ = Mobilized shear force acting on the base; $\alpha_{j,k}$ = Slide angle relative to the $x-y$ plane; α_x , α_y = base inclination in $x-z$ and $y-z$ planes at the middle of each column.

The final safety factor expression for Bishop's simplified method with no groundwater condition is expressed in Eq. (1).

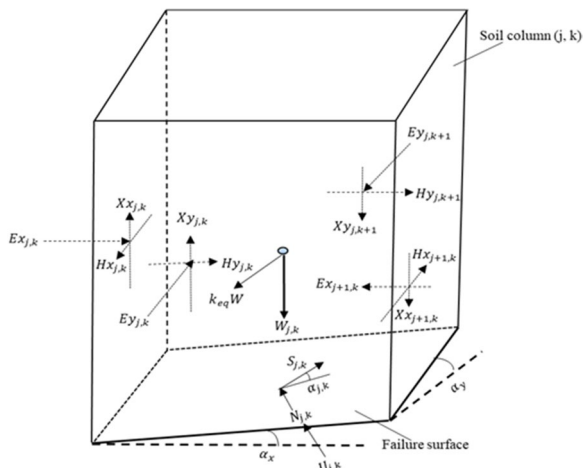


Fig. 3 Free body diagram of j, k column

$$FS = \frac{\sum R_{j,k} (c_{j,k} A_{j,k} + W_{j,k} \tan \phi_{j,k}) / m_{\alpha_{j,k}}}{\sum W_{j,k} [R_{j,k} m_z]} \quad (1)$$

Here, $m_{\alpha_{j,k}} = \cos \varepsilon_{j,k} + \tan \phi_{j,k} m_z$, and $m_z = \sin \alpha_{j,k}$, $c_{j,k}$ = the effective cohesion; $\phi_{j,k}$ = the effective internal friction angle; $R_{j,k}$ is the distance from the j, k column's trial slip region to its axis of rotation; $A_{j,k}$ is the trial surface area of the column; $W_{j,k}$ is the weight of the column; and $\varepsilon_{j,k}$ is the angle between the inclined surface at the bottom of the slice and the horizontal x -axis. For 3D formulation, the summation of normal and shear forces acting along the sides of the columns are assumed to be equal to zero for both the x and y directions.

2.4 Search for critical failure surface and associated FS of 3D slope profile

In Scoops3D, the three-dimensional slope profile is created using the DEM technique. The user inputs the column width, also known as the DEM cell size. DEM input files contain DEM cell surface elevation data. In 3D slope stability analyses, a search method known as Box Search Method is used to find out the critical failure surface and corresponding minimum FS. Figure 4 shows a 3D search lattice of a DEM profile. During the search phase, Scoops3D keeps track of the DEM cells for which the smallest safety factor was determined among all trial surfaces containing that cell. A sphere with a rotatable center point above the DEM and a predetermined radius must contain each trial surface to facilitate the search process. The trial surface with the lowest safety factor is called the critical surface for that DEM cell.

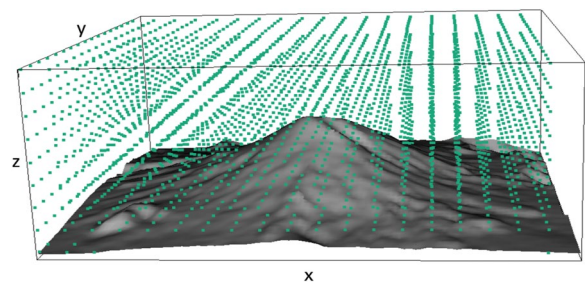


Fig. 4 3D search region of a DEM profile (Source: [49])

2.5 Correlation coefficient of slope height and slope angle with safety factor (FS)

The term correlation coefficient (r) can be defined as the degree of relationship between two variables. Pearson established the Pearson correlation, often known as the correlation coefficient, based on the work of others, including Galton [50], who first found the concept of correlation [51]. The value of the r is always between -1 and +1. Pearson's correlation coefficient (r) is the covariance ratio of two variables to the product of their standard deviations. A positive correlation coefficient indicates if one variable increases, the other value also increases, while a negative correlation coefficient indicates if one variable increases, the other value decreases. A zero-correlation coefficient indicates no relationship between the two variables. The expression of (r) is expressed below:

$$r(x, y) = \frac{\text{cov}(x, y)}{\sigma_x \sigma_y} \quad (2)$$

where cov is the covariance, σ_x is the standard deviation of variable x , and σ_y is the standard deviation of variable y .

The correlation coefficient can be determined using the formula if x and y are the variables under consideration.

$$r = \frac{n(\sum xy) - (\sum x)(\sum y)}{[n \sum x^2 - (\sum x)^2][n \sum y^2 - (\sum y)^2]} \quad (3)$$

where n is the number of variables.

3 Results

Several factors, including soil type and slope geometry, determine the various modes of slope failure. This study investigates the critical failure surface and safety factor for different heights and base inclination angle combinations for three types of soils: clayey, sandy clay, and sandy soil. The soil properties of these soils are shown in Table 1, taken by Shiferaw [3]. To produce the 3D geometric profile of the slope, a DEM input file is prepared.

Table 1 Geotechnical properties of soil

	Clayey	Sandy Clay	Sandy
Cohesion (kPa)	15	5	2
Angle of friction	26	25	33
Unit weight (kN/m ³)	18	16	18

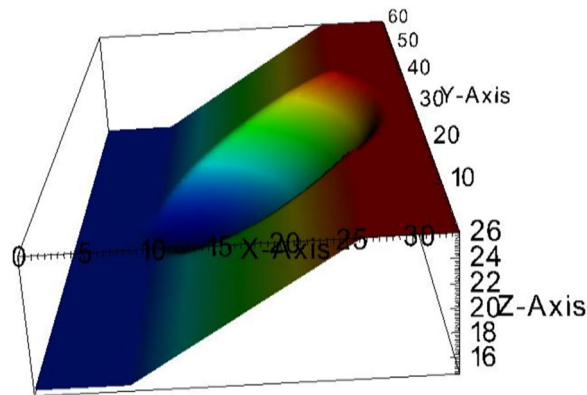


Fig. 5 CFS for Clayey soil (toe slide)

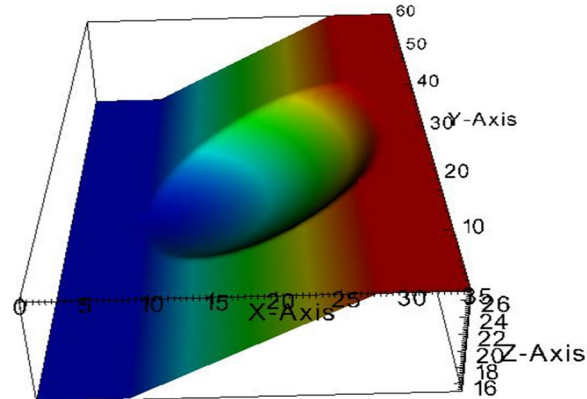


Fig. 6 CFS for Sandy clay soil (toe slide)

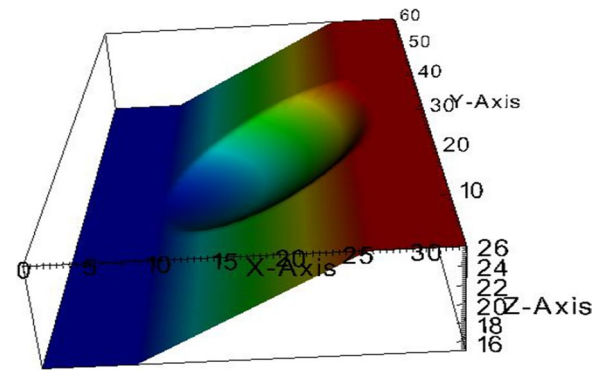


Fig. 7 CFS for Sandy soil (slope/face slide)

Table 2 Critical failure mode based on slope height at slope angle $\beta^\circ = 30.96^\circ$

Slope height (m)	Mode of failure		
	Clayey	Sandy clay	Sandy
12	b	b	c
11	b	b	c
10	b	b	c
9	b	b	c
8	b	b	c
7	b	b	c
6	b	b	c
5	b	b	b
4	b	a	a
3	a	a	a
2	a	a	a
1	a	a	a

(Description of failure mode: a-Base failure, b-Toe failure, c-Slope/Face failure)

The elevation data for the slope’s surface profile are in the DEM file. The horizontal resolution of the DEM grid (m) is taken at 0.50 m intervals. The critical failure surface for a 12 m high and 3 V:5H (30.96°) slope passes through the toe of the slope for clayey and sandy clay soils, while it passes through the slope for sandy soil, as depicted in Figs. 5, 6, and 7, respectively. During 3D slope stability analyses, using sufficient length in the third dimension is important. Other researchers have stated that the length of the third/longitudinal dimension of the slope should not be less than 4H, where H is the height of the slope Chakraborty [52]. The longitudinal/third dimension for 12 m height is 60.0 m, which equals five times the height

of the slope. The three different failure modes occur with height and angle changes. Tables 2 and 3 summarize slope failure modes as slope height and angle change.

3.1 3D Safety factor variation with a slope height

An initial height variation is performed in this study to determine the mode of failure surface and safety factor. The height variation is taken from 12.0 m to 1.0 m at a 1.0 m interval while other parameters have been kept constant. For the three types of soil, the safety factor increases with a decrease in the height of the slope, as shown in Table 4. Shiferaw [3] performed two-dimensional slope stability analyses using PLAXIS-2D for three soil types: clayey, sandy clay, and sandy soils. The 3D slope stability analyses performed for a similar problem reveal that the 3D FS values are 10–20% higher than their 2D values. The differences between 2 and 3D are frequently in the range of 10% to 20% [21, 25, 33]. In this study, the correlation coefficient (r) is carried out

Table 3 Critical failure mode based on slope angle at slope height $H=12$ m

Slope angle (β°)	Mode of failure		
	Clayey	Sandy clay	Sandy
36.86	b	c	c
33.68	b	c	c
30.95	b	c	c
28.60	b	c	c
26.55	b	c	c
24.76	b	c	c
23.2	b	c	c
21.8	b	b	c
20.55	b	b	c
19.44	b	b	c
18.42	a	b	c
17.52	a	b	c

Table 4 3D Safety factor based on slope height at slope angle $\beta^\circ = 30.96^\circ$

Slope height (m)	Safety factor		
	Clayey	Sandy clay	Sandy
12	1.8185	1.2748	1.4194
11	1.8833	1.3072	1.397
10	1.9582	1.3392	1.4023
9	2.0517	1.4867	1.4334
8	2.1643	1.4433	1.4698
7	2.3026	1.5064	1.5179
6	2.4815	1.5923	1.5498
5	2.7251	1.7489	1.7592
4	3.0784	1.8943	1.8329
3	3.7189	2.2917	2.3129
2	5.1413	3.1714	3.2479
1	9.9298	6.1907	6.4056
<i>r</i>	-0.7540	-0.7283	-0.7044

between the height of the slope and the 3D safety factor for all three types of soil, and a negative value is obtained, which indicates a good correlation between the height of the slope and the safety factor.

3.2 3D Safety factor variation with slope angle

The second analytical approach involves gradually changing the slope angle while maintaining the slope height and soil characteristics constant. For the three types of soil, the safety factor increases with a decrease in the slope angle, as shown in Table 5. In this case, a strong

Table 5 3D Safety factor based on slope angle at slope height $H=12$ m

Slope angle (β°)	Safety factor		
	Clayey	Sandy clay	Sandy
36.87	1.6052	1.0944	1.1727
33.69	1.7138	1.1884	1.2688
30.96	1.8185	1.2748	1.4194
28.61	1.925	1.3674	1.4832
26.56	2.0246	1.4536	1.595
24.78	2.1317	1.5512	1.7235
23.2	2.231	1.6448	1.8741
21.8	2.332	1.741	2
20.56	2.4367	1.8391	2.1236
19.44	2.5462	1.9437	2.2511
18.43	2.6634	2.0526	2.3827
17.53	2.7836	2.1628	2.5139
<i>r</i>	-0.9793	-0.9747	-0.9726

opposite correlation coefficient was found between the slope angle and 3D safety factor for three soil types.

3.3 3D Safety factor variation with slope height and angle

In a third analysis, the author investigated different slope height and angle combinations while keeping the soil parameters the same. This analysis finds slope heights of 12 m, 9 m, 6 m, and 3 m. The slope angle considered for each slope height is $30.96^\circ, 25.64^\circ, 21.8^\circ,$ and $18.77^\circ,$ respectively. In this analysis, sandy clay soil is the only type of soil considered for analysis. The calculated safety factor value for the third analysis is shown in Table 6. The reported 3D safety factor values for sandy clay with slope and height variation are compared to the 2D safety factor [3]. So, the increase in safety factor values is observed at 10–20% compared to 2D slope analysis.

4 Discussion

Shiferaw [3] performed two-dimensional slope stability analyses using PLAXIS-2D for three soil types: clayey, sandy clay, and sandy soils. The 3D slope stability analyses performed for a similar problem reveal that the 3D FS values are 10–20% higher than their 2D values.

4.1 The effect of slope angle and height on the failure mode of slope

Slope failure can occur in three ways: slope/face failure, toe slide, and base slide. Both the kind of soil and the slope’s geometry influence the failure mode. Tables 2 and 3 show that the slopes fail differently depending on their height and angle. Toe slide is the most common slope

Table 6 3D safety factor based on Height and Angle of slope

Height (m)	Angle (β°)	Safety factor of Sandy clay		
		Present Study 3D	Shiferaw [3] 2D	% Increase
12	30.96	1.2748	1.151	10.76
12	25.64	1.4962	1.3855	7.99
12	21.8	1.7206	1.6028	7.35
12	18.77	1.9733	1.8047	9.34
9	30.96	1.4867	1.2546	18.50
9	25.64	1.6242	1.5019	8.14
9	21.8	1.8375	1.7233	6.63
9	18.77	2.0749	1.9299	7.51
6	30.96	1.5923	1.4433	10.32
6	25.64	1.8237	1.713	6.46
6	21.8	2.0589	1.9315	6.60
6	18.77	2.3004	2.1485	7.07
3	30.96	2.2917	0.9494	17.56
3	25.64	2.4901	2.2387	11.23
3	21.8	2.6696	2.4882	7.29
3	18.77	2.9051	2.7344	6.24

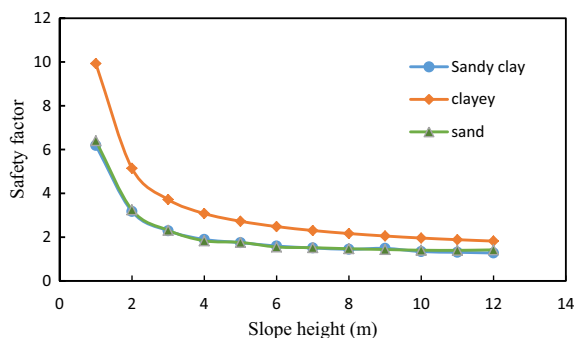


Fig. 8 Safety factor vs. slope height

failure on clay and sandy soils. The most common type of failure in sandy soil is a slope/face slide. In this study, all three soil types: clayey, sandy clay, and sandy soil, fail by base sliding at heights less than 4 m.

Slope/face slide failure is typical for sandy clay soils on steep slopes, while toe slide failure dominates on mild slopes. Toe sliding is the predominant mode of failure for clayey soils. The base slide happens when the slope angle is less than 18° . In sandy soil conditions, slope/face slides are the most typical form of failure.

4.2 The effect of slope height on safety factor

When the slope height increases in the later stage, there is a general trend toward a slower rate of rise in the safety factor. Figure 8 shows that the safety factor increases quickly for height changes of less than 3 m. Figure 8 depicts a reasonably steady slope of the line for a range

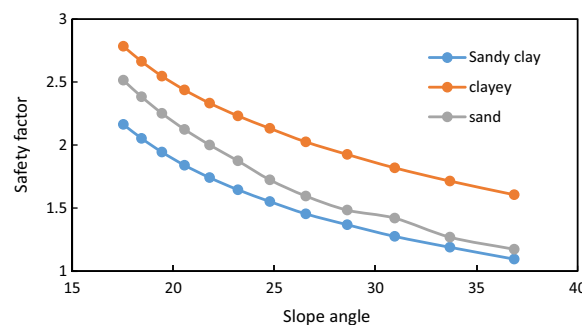


Fig. 9 Safety factor vs. slope angle

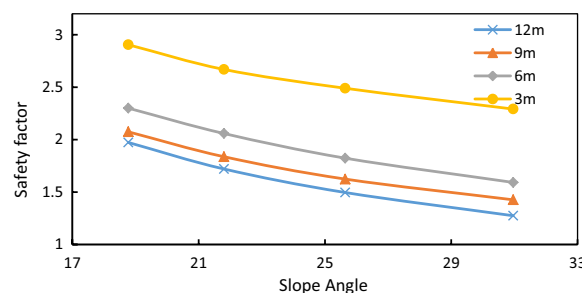


Fig. 10 Slope angle vs. safety factor for different slope heights

of slope heights from 12 m down to 4 m. The correlation examination reveals a significant negative linear relationship between slope height and FS, with $r = -0.96159$. Observe the abrupt shift in the slope of the graph between height and safety factor at 3 m. Correlation analysis between 3 and 1 m heights yields $r = -0.95437$. The overall r is -0.7540 , which means the safety factor decreases slower as height goes from 12 to 3 m. After a slope is 3 m high, the safety factor increases faster.

4.3 Slope angle's effect on the safety factor

As the slope gets steeper, the safety factor drops almost in a straight line. Figure 9 demonstrates that the correlation between the slope angle and the safety factor is almost straight while the angle gets steeper. The correlation coefficient between the slope angle and the safety factor is -0.9793 . According to the correlation coefficient, there is a significant and inverse association between slope angle and FS for the three types of soil.

4.4 The effect of slope height and slope on safety factor

The safety factor can be maximized by optimizing slope height and angle. Calculating the FS shown in Table 6 allows researchers to examine the effects of decreasing slope height and angle. As shown in Fig. 10, a slope height of 3 m or less increases the FS at a higher rate than

a height of 3 m or more. So, decreasing the slope angle on slopes with less height increases the FS at a higher rate.

Figure 11 illustrates the difference in the FS with respect to height at various slope angles. When slope height increases, the safety factor decreases. Further, it is seen that the safety factor increases when the slope angle decreases.

The variation of FS with slope's height and base angle has been earlier studied by Shiferaw [3]. In two dimensions, in 3D, the authors could not find any similar study. Therefore, it is difficult to compare these results with previously published results.

5 Conclusions

The present study is useful for investigating the variation of the safety factor of a three-dimensional homogenous soil slope subjected to self-weight only. The results indicate that the slope's height and angle influence how the three soil types fail. Toe slip is the predominant slope collapse for clay and sandy clay soils. It is noticed that for sandy soil, slope failure is the dominant mode of failure. All three soil types: clayey, sandy clay, and sandy soil, fail due to base sliding at heights below 4.0 m. Sandy clay soils collapse by slope slide on steep slopes and toe slide on mild slopes. Clayey soils fail mostly by toe sliding. Slopes under 18° cause base slides. Most sandy soil failures are slope/face slides. Slope safety generally increases linearly as the slope angle decreases, although the safety factor rises at variable rates as the slope height decreases. Slope heights under 3.0 m raise safety factors faster than those over 3.0 m. Thus, decreasing the slope angle on lower slope height enhances the safety factor. The expected failure type will be either toe or face failure when the slope's height and base angle exceeds 5.0 m and 22° , respectively. This study also found that the three-dimensional safety factor for soil slope is generally 10–20% higher than the two-dimensional factor of slope safety. The correlation coefficient shows a strong inverse

correlation between the safety factor and slope angle. Knowing the failure mode and the influence of geometric change on the slope safety factor can help researchers choose the best method for improving slope stability. The study can be further extended to observe the variation of the FS for a 3D slope subjected to pore water pressure and seismic loading.

Abbreviations

FS Factor of safety
DEM Digital elevation model

Acknowledgements

The authors thank Nit Patna's colleagues for their kind support in this work

Author contributions

All author who contributed to the whole work. The authors read and approved the final manuscript.

Funding

None.

Availability of data and materials

All the data is available in the manuscript.

Declarations

Ethics approval and consent to participate

Not applicable.

Consent for publication

Not applicable.

Competing interests

The authors declare that they have no competing interests.

Received: 6 February 2023 Accepted: 13 September 2023

Published online: 21 September 2023

References

- Pourkhosravani A, Kalantari B (2011) A review of current methods for slope stability evaluation. *Electron J Geotech Eng* 16:1245–1254
- Chatterjee D, Murali Krishna A (2019) Effect of slope angle on the stability of a slope under rainfall infiltration. *Indian Geotech J* 49:708–717
- Shiferaw HM (2021) Study on the influence of slope height and angle on the factor of safety and shape of failure of slopes based on strength reduction method of analysis. *Beni-Suef Univ J Basic Appl Sci* 10:1–11
- Rotaru A, Oajdea D, Răileanu P (2007) Analysis of the landslide movements. *Int J Geol* 1:70–79
- Petley DN, Bulmer MH, Murphy W (2002) Patterns of movement in rotational and translational landslides. *Geology* 30:719–722
- Kumar DR, Samui P, Wipulanusat W et al (2023) Soft-computing techniques for predicting seismic bearing capacity of strip footings in slopes. *Buildings* 13:1371
- Fellenius W (1936) Calculation of stability of earth dam. In *Transactions. 2nd Congress Large Dams*. 4:445–462
- Bishop AW (1955) THE USE OF THE SLIP CIRCLE IN THE STABILITY ANALYSIS OF SLOPES. *First Tech Sess Gen Theory Stab Slopes*
- Spencer E (1967) A method of analysis of the stability of embankments assuming parallel inter-slice forces. *Geotechnique* 17:11–26
- Mongemstern NR, Price VE (1965) The Analysis of stability of general slide surfaces. *Geotechnique* 15:79–93

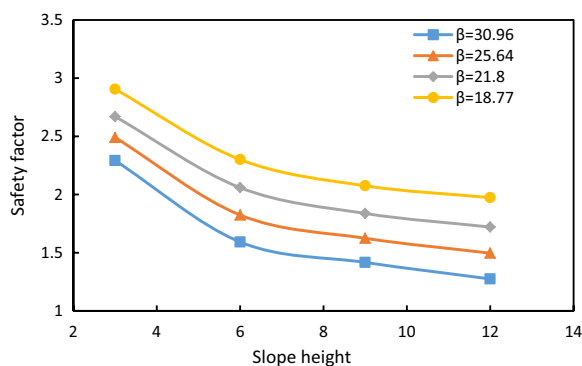


Fig. 11 Slope height vs. safety factor for slope angle

11. Sarma SK (1973) Stability analysis of embankments and slopes. *Geotechnique* 23:423–433
12. Janbu N (1973) Slope stability computations. Publ Wiley Sons, Inc
13. Singh P, Bardhan A, Han F et al (2023) A critical review of conventional and soft computing methods for slope stability analysis. *Model Earth Syst Environ* 9:1–17
14. Kalatehjari R, Rashid ASA, Hajihassani M et al (2014) Determining the unique direction of sliding in three-dimensional slope stability analysis. *Eng Geol* 182:97–108
15. Lam L (1993) A general limit equilibrium model for three-dimensional slope stability analysis. *Canadian Geotech J* 30(6):905–919
16. Chen RH, Chameau J (1982) Three-dimensional limit equilibrium analysis of slopes. *Geotechnique* 33(1):31–40
17. Li H, Shao L (2011) Three-dimensional finite element limit equilibrium method for slope stability analysis based on the unique sliding direction. In: *Slope Stability and Earth Retaining Walls*. pp 48–55
18. Rao B, Burman A, Roy LB (2023) An Efficient Box Search Method for Limit Equilibrium Method-Based 3D Slope Stability Analysis. *Transp Infrastruct Geotechnol* 1–32
19. Leshchinsky D, Huang CC (1992) Generalized slope stability analysis: interpretation modification and comparison. *J Geotech Eng* 118:1559–1576
20. Baligh MM, Azzouz AS (1975) End effects on stability of cohesive slopes. *J Geotech Eng Div* 101:1105–1117
21. Hovland HJ (1977) Three-dimensional slope stability analysis method. *J Geotech Eng Div* 103:971–986
22. Hungr O, Salgado FM, Byrne PM (1989) Evaluation of a three-dimensional method of slope stability analysis. *Can Geotech J* 26:679–686. <https://doi.org/10.1139/t89-079>
23. Leshchinsky D, Baker R, Silver ML (1985) Three dimensional analysis of slope stability. *Int J Numer Anal Methods Geomech* 9:199–223
24. Leshchinsky D, Huang C-C (1992) Generalized slope stability analysis: Interpretation, modification, and comparison. *J Geotech Eng* 118:1559–1576
25. Xing Z (1988) Three-dimensional stability analysis of concave slopes in plan view. *J Geotech Eng* 114:658–671
26. Ugai K (1985) Three-dimensional stability analysis of vertical cohesive slopes. *Soils Found* 25:41–48
27. Hungr O (1987) An extension of Bishop's simplified method of slope stability analysis to three dimensions. *Geotechnique* 37:113–117
28. Lam L, Fredlund DG (1994) A general limit equilibrium model for three-dimensional slope stability analysis: Reply. *Can Geotech J* 31:795–796. <https://doi.org/10.1139/t94-094>
29. Yamagami T, Jiang J (1997) A search for the critical slip surface in three-dimensional slope stability analysis. *Soils Found* 37:1–16
30. Huang C-C, Tsai C-C (2000) New method for 3D and asymmetrical slope stability analysis. *J Geotech Geoenviron Eng* 126:917–927
31. Huang C, Tsai C, Chen Y (2002) Generalized method for three-dimensional slope stability analysis. *J Geotech Geoenviron Eng* 128(10):836–848
32. Cheng YM, Yip CJ (2007) Three-dimensional asymmetrical slope stability analysis extension of bishop 's, Janbu 's, and Morgenstern – price 's techniques. *J Geotech Geoenviron Eng* 133:1544–1555
33. Duncan JM (1996) State of the art: limit equilibrium and finite-element analysis of slopes. *J Geotech Eng* 122:577–596
34. Kumar S, Choudhary SS, Burman A (2022) Recent advances in 3D slope stability analysis: a detailed review. *Model Earth Syst Environ* 9(2):1445–1462
35. Xu Q, Lu Y, Yin H, Li Z (2010) Element Integration Method for upper bound limit analysis. *Mech Res Commun* 37:611–616
36. Chen W (1975) Limit analysis and soil plasticity Elsevier
37. Lysmer J (1970) Limit analysis of plane problems in soil mechanics. *J Soil Mech Found Div* 96:1311–1334
38. Michalowski RL (1995) Slope stability analysis: a kinematical approach. *Geotechnique* 45:283–293
39. Michalowski RL (2002) Stability charts for uniform slopes. *J Geotech Geoenviron Eng* 128:351–355
40. Loukidis D, Bandini P, Salgado R (2003) Comparative study of limit equilibrium, limit analysis and finite element analysis of the seismic stability of slopes. *Geotechnique* 53:463–479
41. Yu HS, Salgado R, Sloan SW, Kim JM (1998) Limit analysis versus limit equilibrium for slope stability. *J Geotech Geoenviron Eng* 124:1–11
42. Giger MW, Krizek RJ (1975) Stability analysis of vertical cut with variable corner angle. *Soils Found* 15:63–71
43. De Buhan P, Garnier D (1998) Three dimensional bearing capacity analysis of a foundation near a slope. *Soils Found* 38:153–163
44. Cheng YM, Lansivaara T, Wei WB (2007) Two-dimensional slope stability analysis by limit equilibrium and strength reduction methods. *Comput Geotech* 34:137–150
45. Tschuchnigg F, Schweiger HF, Sloan SW et al (2015) Comparison of finite-element limit analysis and strength reduction techniques. *Géotechnique* 65:249–257
46. Ugai K (1988) Three-dimensional slope stability analysis by slice methods. In: *Proc. 6th Inter. Conf. on Numer. Meth. in Geomech., Innsbruck, Austria, 1988*
47. Baker R, Leshchinsky D (1987) Stability analysis of conical heaps. *Soils Found* 27:99–110
48. ASCE (2013) Policy statement 418—The role of the civil engineer in sustainable development
49. Reid ME, Christian SB, Brien DL, Henderson S (2015) Scoops3D—software to analyze three-dimensional slope stability throughout a digital landscape. *US Geol Surv Tech Methods*, B 14:
50. Galton F (1889) I. Co-relations and their measurement, chiefly from anthropometric data. *Proc R Soc London* 45:135–145
51. Lee Rodgers J, Nicewander WA (1988) Thirteen ways to look at the correlation coefficient. *Am Stat* 42:59–66
52. Chakraborty A, Goswami D (2021) Three-dimensional (3D) slope stability analysis using stability charts. *Int J Geotech Eng* 15:642–649

Publisher's Note

Springer Nature remains neutral with regard to jurisdictional claims in published maps and institutional affiliations.

Submit your manuscript to a SpringerOpen[®] journal and benefit from:

- Convenient online submission
- Rigorous peer review
- Open access: articles freely available online
- High visibility within the field
- Retaining the copyright to your article

Submit your next manuscript at ► [springeropen.com](https://www.springeropen.com)